

## Efficient Multistep Photoinitiated Electron Transfer in a Molecular Pentad

DEVENS GUST,\* THOMAS A. MOORE,\* ANA L. MOORE,\* SEUNG-JOO LEE, EDITH BITTERS-MANN, DAVID K. LUTTRULL, ADEN A. REHMS, JANICE M. DEGRAZIANO, XIAOCHUN C. MA, FENG GAO, ROBERT E. BELFORD, TODD T. TRIER

A synthetic five-part molecular device has been prepared that uses a multistep electron transfer strategy similar to that of photosynthetic organisms to capture light energy and convert it to chemical potential in the form of long-lived charge separation. It consists of two covalently linked porphyrin moieties, one containing a zinc ion ( $P_{Zn}$ ) and the other present as the free base (P). The metallated porphyrin bears a carotenoid polyene (C) and the other a diquinone species ( $Q_A$ - $Q_B$ ). Excitation of the free-base porphyrin in a chloroform solution of the pentad yields an initial charge-separated state,  $C-P_{Zn}-P^+-Q_A^--Q_B$ , with a quantum yield of 0.85. Subsequent electron transfer steps lead to a final charge-separated state,  $C^+-P_{Zn}-P-Q_A-Q_B^-$ , which is formed with an overall quantum yield of 0.83 and has a lifetime of 55 microseconds. Irradiation of the free-base form of the pentad,  $C-P-P-Q_A-Q_B$ , gives a similar charge-separated state with a lower quantum yield (0.15 in dichloromethane), although the lifetime is increased to  $\sim 340$  microseconds. The artificial photosynthetic system preserves a significant fraction ( $\sim 1.0$  electron volt) of the initial excitation energy (1.9 electron volts) in the long-lived, charge-separated state.

NATURAL PHOTOSYNTHETIC REACTION centers exploit solar power by collecting light energy and using it to separate charge across a lipid bilayer membrane. The transmembrane electron transfer is accomplished in the reaction center protein environment by a series of short-range, fast, and efficient steps. The resulting charge-separated state is long-lived, in part because the relatively large distance between the positive and negative charges retards direct recombination. We have investigated this multistep electron transfer strategy in three- and four-part molecules consisting of covalently linked porphyrins, carotenoids, and quinones (1). The knowledge gained from these simpler systems has now allowed the design and synthesis of molecular pentad **1** (Fig. 1). This structure features a diporphyrin moiety ( $P_{Zn}$ -P) covalently linked to a carotenoid polyene (C) and a diquinone structure ( $Q_A$ - $Q_B$ ). The porphyrin bearing the carotenoid is metallated with zinc, whereas the other is in the free-base form (2).

The absorption spectrum of **1** in chloroform is nearly identical to the sum of the

spectra of unlinked model chromophores. The fluorescence emission spectrum in the same solvent has maxima at 655 and 718 nm. These bands are typical of emission from free-base porphyrins. However, the emission is quenched relative to that of model carotenoporphyrin compounds that lack the diquinone moiety. In addition, a very weak band, characteristic of emission from a zinc porphyrin, appears at 611 nm. The quenching of the steady-state fluorescence suggests that, in common with those of other porphyrin-quinone systems (3), the free-base porphyrin singlet state is being quenched by electron transfer to the quinone to generate  $C-P_{Zn}-P^+-Q_A^--Q_B$ . In addition, the lack of strong emission from the zinc porphyrin moiety of **1** is consistent with rapid singlet energy transfer to the free-base porphyrin. We undertook time-resolved fluorescence studies to investigate these possibilities.

Fluorescence decay curves were obtained

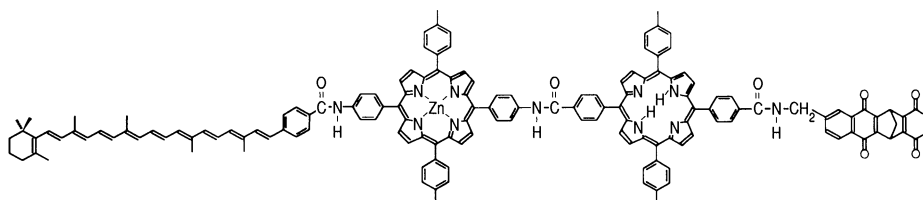


Fig. 1. Molecular structure of pentad **1**.

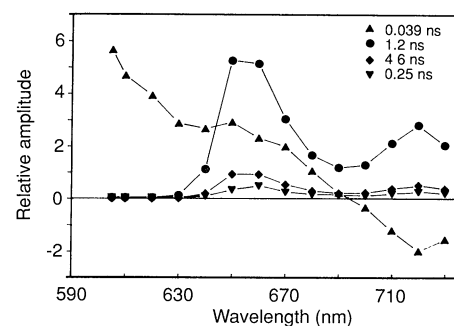


Fig. 2. Results of a global analysis of the decay of the porphyrin fluorescence of pentad **1** after excitation of a  $\sim 1 \times 10^{-6} M$  chloroform solution with a laser pulse at 590 nm. Data were obtained by use of the single-photon counting technique. The instrument response was  $\sim 0.035$  ns. Decays at the 14 different wavelengths were analyzed simultaneously to fit the data to four exponential functions. The goodness-of-fit parameter  $\chi^2$  was 1.12. Satisfactory fits were not obtained with fewer exponential functions.

by the single-photon counting technique (4). The results for **1** in chloroform are shown in Fig. 2. The sample was excited at 590 nm, and emission decay curves were taken at 14 wavelengths. We fitted all 14 decays simultaneously to four exponentials ( $\chi^2 = 1.12$ ), using a global analysis technique (5) that yields the decay-associated spectra shown in the figure. The two major components of the decay had lifetimes of  $0.039 \pm 0.005$  and  $1.2 \pm 0.05$  ns. (The two minor components, 4.6 and 0.25 ns, represent impurities or conceivably a minor conformer in the case of the 4.6-ns decay.) Excitation at 650 nm yielded similar decay-associated spectra that lacked the 0.039-ns component.

In order to discuss the origins of these decay components, it is useful to refer to Fig. 3, which depicts the relevant high-energy states of **1** and some of the pathways available for their interconversion. The excited singlet-state energies were calculated from the absorption and fluorescence emission spectra. The energies of the various charge-separated states were estimated from cyclic voltammetric studies of models for the components of the pentad (carotenoid, porphyrins, diquinone). The energy levels in Fig. 3 are not corrected for any coulombic stabilization of the intermediates.

Returning to an examination of Fig. 2, we see that the 0.039-ns component comprises

Department of Chemistry and Center for the Study of Early Events in Photosynthesis, Arizona State University, Tempe, AZ 85287.

\*To whom correspondence should be addressed.

essentially the sole emission in the 610-nm region, where only the zinc porphyrin fluoresces, and manifests itself as a negative component (rise time) in the 710-nm region, where most of the emission comes from the free-base porphyrin. The decay in the 610-nm region reflects the decay of the zinc porphyrin singlet state, and the corresponding rise in emission intensity in the 710-nm region signifies the population of the free-base porphyrin singlet state by energy transfer from  $P_{Zn}$  (step 1 in Fig. 3). A model carotenoid-bearing zinc porphyrin, in which there is no possibility of such energy transfer, has a singlet lifetime of  $0.37 \pm 0.05$  ns. Thus, if it is assumed that the addition of the free-base porphyrin serves only to introduce the possibility of energy transfer, the singlet energy transfer rate constant  $k_1$  may be calculated as follows:

$$k_1 = (1/0.039 \times 10^{-9}) - (1/0.37 \times 10^{-9}) = 2.3 \times 10^{10} \text{ s}^{-1} \quad (1)$$

The quantum yield for energy transfer, given by  $k_1/(1/0.039 \times 10^{-9})$ , is 0.90.

The 1.2-ns component (Fig. 2) has a spectrum consistent with emission from the free-base porphyrin. Singlet states of similar porphyrins under these conditions, with or without an attached zinc porphyrin moiety but lacking attached quinones, have lifetimes of 7.8 ns. The addition of the quinone opens up a new pathway for decay of the porphyrin singlet state: electron transfer to the quinone to generate  $C-P_{Zn}-P^{+}-Q_A^{-}-Q_B^{-}$  (step 2 in Fig. 3). The rate constant for this photoinitiated electron transfer may therefore be estimated as:

$$k_2 = (1/\tau) - (1/\tau_0) \quad (2)$$

where  $\tau$  is the fluorescence lifetime of the free-base porphyrin singlet state and  $\tau_0$  is the lifetime of a model compound with photo-physics similar to those of **1** but without the electron transfer step (that is, 7.8 ns). Thus,

$k_2$  equals  $7.1 \times 10^8 \text{ s}^{-1}$ . The corresponding quantum yield is  $k_2/(1/\tau)$  or 0.85.

Given the formation of  $C-P_{Zn}-P^{+}-Q_A^{-}-Q_B^{-}$ , studies of simpler but related molecular devices (6, 7) suggest that two secondary electron transfer reactions, steps 3 and 4 in Fig. 3, should compete with charge recombination to the ground state (step 10). Step 3 involves electron transfer from the naphthoquinone moiety to the benzoquinone (a better electron acceptor) to yield  $C-P_{Zn}-P^{+}-Q_A^{-}-Q_B^{-}$ . Two subsequent electron transfers (steps 7 and 8) lead to a final charge-separated state  $C^{+}-P_{Zn}-P-Q_A^{-}-Q_B^{-}$ . Alternatively, step 4, which involves electron transfer from the zinc porphyrin to the free-base radical cation, generates  $C-P_{Zn}^{+}-P-Q_A^{-}-Q_B^{-}$ , which can also decay to  $C^{+}-P_{Zn}-P-Q_A^{-}-Q_B^{-}$  by two different pathways. Thus, the pentad has been constructed so that all of the likely electron transfer pathways converge to the same final  $C^{+}-P_{Zn}-P-Q_A^{-}-Q_B^{-}$  state, in which the electron and the hole are located at opposite ends of the molecule.

Transient absorption studies on the nanosecond time scale (8, 9) reveal that this state is indeed produced. Excitation of the free-base porphyrin moiety of **1** in chloroform solution at 650 nm resulted in the observation of a long-lived transient (Fig. 4), which was identified by its spectrum (maximum wavelength = 970 nm) as the carotenoid radical cation (10). This transient represents  $C^{+}-P_{Zn}-P-Q_A^{-}-Q_B^{-}$ . The decay was fitted as a single exponential to yield a lifetime of 55  $\mu\text{s}$ . The quantum yield of the charge-separated state, estimated by the comparative method (11, 12), was  $\sim 0.83$ . Thus, the yield of the steps from  $C-P_{Zn}-P^{+}-Q_A^{-}-Q_B^{-}$  to the final state is essentially quantitative. Determination of the relative contributions of the various electron transfer pathways in Fig. 3 to the total yield must await transient absorption studies on the picosecond time

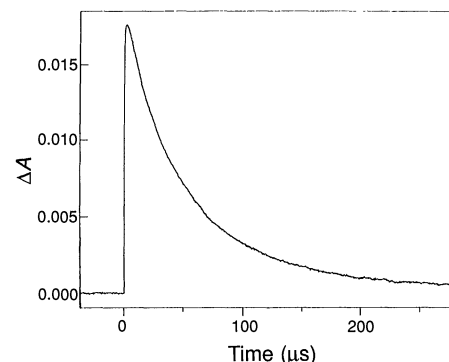
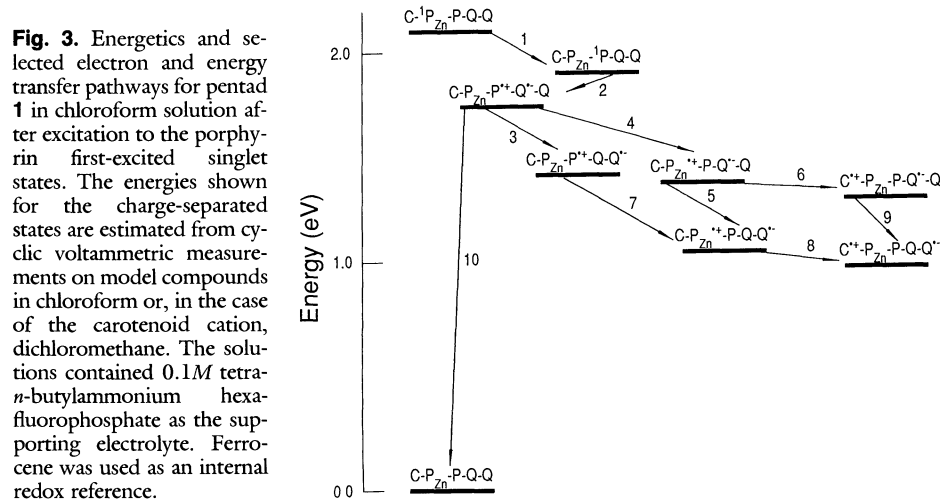


**Fig. 4.** Decay of the transient absorption at 970 nm after laser flash excitation of pentad **1** ( $\sim 5 \times 10^{-6} M$  in chloroform solution) at 650 nm. The species giving rise to the transient is the charge-separated state  $C^{+}-P_{Zn}-P-Q_A^{-}-Q_B^{-}$ . A three-parameter fit of the decay (floating baseline) yields a lifetime of  $\tau = 55 \mu\text{s}$  (10). The overall quantum yield of  $C^{+}-P_{Zn}-P-Q_A^{-}-Q_B^{-}$  is  $\sim 0.83$ .

scale. However, comparison of the results for **1** with those for our earlier model systems (1) suggests that it is the thermodynamically favorable interporphyrin electron transfer step 4 that is mainly responsible for the enhanced quantum yield of charge separation for **1**. This pathway, which competes well with the initial charge recombination, was not available in the previous systems.

Pentad **1** shows similar behavior in dichloromethane solution. The rate constant for energy transfer is essentially unchanged at  $2.5 \times 10^{10} \text{ s}^{-1}$ , but the rate constant for step 2 is reduced to  $2.9 \times 10^8 \text{ s}^{-1}$ . Consequently, the quantum yield of this step is reduced to 0.71. Such a decrease in the rate constant for photoinitiated electron transfer when the solvent is changed from chloroform to dichloromethane has been reported in porphyrin-quinone dyad systems (13). Transient absorption studies with excitation at 650 nm show that the subsequent electron transfer steps yield  $C^{+}-P_{Zn}-P-Q_A^{-}-Q_B^{-}$  with a quantum yield of  $\sim 0.60$ . The lifetime of the final state, however, is increased to  $\sim 200 \mu\text{s}$ .

The analog of **1** in which both porphyrins are present as the free base also demonstrates photoinitiated electron transfer to yield a long-lived, charge-separated state. In this case the quantum yield of  $C^{+}-P-P-Q_A^{-}-Q_B^{-}$  in dichloromethane is only 0.15, but the lifetime of this state is  $\sim 340 \mu\text{s}$ . There are two reasons for the reduced quantum yield for this molecule relative to **1**. In the first place, although the rate constant for step 2 ( $2.3 \times 10^8 \text{ s}^{-1}$ ) is similar to that found for **1**, the quantum yield for this step is reduced to 0.35 because of an increased rate of decay of the porphyrin singlet by other pathways. In addition, the interporphyrin electron transfer step 4 competes less efficiently with charge recombination because the  $C-P^{+}-P-$



$Q_A^{\cdot-}-Q_B$  state is destabilized by  $\sim 0.2$  eV relative to  $C-P_{Zn}^{\cdot+}-P-Q_A^{\cdot-}-Q_B$ .

The lifetimes of the final charge-separated states in these pentad molecules are far longer than those observed for the simpler three- and four-part molecular devices that we have reported (1) but are substantially shorter than would be expected for direct charge recombination, on the basis of the results for related species. In this connection, it should be noted that in simpler triad systems, charge recombination occurs by a two-step reaction involving an intermediate species (8). A related mechanism may be operating here, although more studies will be necessary in order to elucidate the details of the process.

Although pentad 1 and related molecules differ significantly in structure from natural reaction centers, they do mimic several aspects of photosynthetic energy conversion. These include rapid singlet energy transfer to the primary donor, triplet energy transfer to the carotenoid, and a multistep electron transfer strategy that achieves efficient long-range and long-lived charge separation. There remain many important unanswered questions concerning natural photosynthesis that these artificial systems do not address or fail to mimic. However, pentad 1 does demonstrate that compounds can be designed in which electron transfer after photoexcitation occurs over several redox centers with a yield of near unity while conserving more than one-half of the excited-state energy of the primary donor. Thus, it appears that there is no a priori reason why the essential features of photosynthetic solar energy conversion cannot ultimately be reproduced successfully with man-made molecular devices (14).

#### REFERENCES AND NOTES

1. For a recent review, see D. Gust and T. A. Moore, *Science* **244**, 35 (1989).
2. The synthesis and characterization of this material will be reported elsewhere.
3. For a comprehensive review, see J. S. Connolly and J. R. Bolton, in *Photoinduced Electron Transfer*, Part D, M. A. Fox and M. Channon, Eds. (Elsevier, Amsterdam, 1988), chap. 6.2.
4. D. Gust *et al.*, *Photochem. Photobiol.*, in press.
5. J. Wandler and A. R. Holzwarth, *Biophys. J.* **52**, 717 (1987).
6. D. Gust *et al.*, *J. Am. Chem. Soc.* **110**, 321 (1988).
7. D. Gust *et al.*, *ibid.*, p. 7567.
8. D. Gust *et al.*, *ibid.* **108**, 8028 (1986).
9. F. S. Davis *et al.*, *Rev. Sci. Instrum.* **58**, 1629 (1987).
10. At 960 nm, the transient signal rises to  $\sim 90\%$  of its maximum value with the response time of the instrument and reaches the peak value within several microseconds.
11. R. Bensasson, C. R. Goldschmidt, E. J. Land, T. G. Truscott, *Photochem. Photobiol.* **28**, 277 (1978). Quantum yields are based on published extinction coefficients for transient species (carotenoid radical cations and porphyrin triplet states), which are not accurately known (12). Excitation at 590 nm reduced the observed quantum yield to about 0.45. This wavelength-dependent quantum yield of charge separation is unusual; it does not occur in the

nonmetallated pentad and will be the subject of a future report (D. Gust *et al.*, in preparation).

12. T. A. Moore *et al.*, *Nature* **307**, 630 (1984).
13. J. A. Schmidt, A. Siemiarzuk, A. C. Weedon, J. R. Bolton, *J. Am. Chem. Soc.* **107**, 6112 (1985).
14. G. Ciamician, *Science* **36**, 385 (1912).
15. This work was supported by the Division of Chemical Sciences, Office of Basic Energy Sciences, Office of Energy Research, U.S. Department of Energy (DE-FG02-87ER13791) and the Department of

Energy University Research Instrumentation Program (DE-FG05-87ER75361). This is publication 43 from the Arizona State University Center for the Study of Early Events in Photosynthesis. The Center is funded by U.S. Department of Energy grant DE-FG02-88ER13969 as part of the U.S. Department of Agriculture-Department of Energy-National Science Foundation Plant Science Center Program.

10 October 1989; accepted 8 February 1990

## Primary Sequence Information from Intact Proteins by Electrospray Ionization Tandem Mass Spectrometry

JOSEPH A. LOO, CHARLES G. EDMONDS, RICHARD D. SMITH\*

Tandem mass spectrometry has been used to obtain information related to portions of the primary sequence for an intact protein, bovine ribonuclease A. Multiply charged molecular ions, generated by electrospray ionization, were collisionally dissociated at low energies in a triple quadrupole mass spectrometer to yield singly and multiply charged fragment ions that can be assigned to the known sequence of the protein. Dissociation of the highly charged molecular ions resulted in pairs of complementary product ions. The higher order (gas-phase) protein structure affects the dissociation processes, as observed in comparisons of tandem mass spectra of the native and disulfide-reduced forms of ribonuclease A.

MASS SPECTROMETRY (MS) AND tandem mass spectrometry (MS/MS) can be important tools in the determination of primary peptide and protein structure (1), especially for proteins that are blocked for conventional sequence analysis, that have undergone posttranslational modifications, or that are available only in small (picomole) quantities (2). However, facile MS analysis of larger polypeptides and proteins (molecular weights,  $M_r$ , greater than  $\sim 4000$ ) will require the ability not only to form the gas-phase ions of the parent molecule, but also to cause the parent ion to undergo fragmentation processes so that sequence-related information can be obtained.

We report collision-induced dissociation (CID) tandem mass spectra for a multiply protonated intact protein, ribonuclease A (RNase A), produced by electrospray ionization (ESI), and demonstrate the feasibility of sequence-specific assignment of the product ion spectra. This analysis is accomplished, in part, by experimental methods that verify tentative CID product ion assignments based upon subsequent CID steps. Significant differences are found in MS/MS spectra of the native and reduced forms of RNase A, that is, after cleavage of disulfide bonds, suggesting that CID pro-

cesses are influenced by secondary or tertiary protein structure.

Although a number of competing methods exist for ionizing proteins, such as plasma desorption (PD) (3), laser desorption (4), and fast-atom bombardment (FAB) (5), ESI-MS shows potential as the method of choice for sensitive, rapid, and accurate molecular weight determination of large biomolecules (6-8) requiring as little as femtomole quantities (7). The atmospheric-pressure ESI source produces multiply charged (protonated) molecular ions from highly charged liquid droplets for proteins exceeding 100 kD; ions bearing more than 100 positive charges per molecule have been observed (7).

Tandem MS (9) has been used to determine primary structure for oligopeptides and, indirectly, proteins. The CID processes yield product ions characteristic of the amino acid sequence. More important, a range of possible modifications of oligopeptides can often be ascertained with speed and reliability (2, 10). Highly specific enzymatic digests of proteins followed by MS (FAB peptide mapping) and MS/MS of the peptide mixture can aid sequence determination of proteins (2, 10). Biemann (2) has discussed and demonstrated the enhanced speed of peptide and protein sequencing by such MS methods relative to conventional Edman degradation procedures (one residue per minute versus one residue per hour). High-performance liquid chromatography (HPLC) is often used to separate complex peptide mixtures to simplify the method

Chemical Methods and Separations Group, Chemical Sciences Department, Pacific Northwest Laboratory, Richland, WA 99352.

\*To whom correspondence should be addressed.